Environmental Science Nano

Filtration-based water treatment system embedded with black phosphorus for NIR-triggered disinfection

Journal:	*Environmental Science: Nano*
Manuscript ID	EN-ART-07-2019-000774.R1
Article Type:	Paper
Date Submitted by the Author:	14-Aug-2019

Complete List of Authors:	Li, Dengyu; Institute of Applied Ecology Chinese Academy of Sciences Zhao, Qing; Institute of Applied Ecology, CAS Zhang, Siyu; Dalian University of Technology, School of Environmental Science and Technology; Chinese Academy of Science, Institute of Applied Ecology Wu, Fengchang; Chinese Research Academy of Environmental Sciences Yu, Xuefeng; Shenzhen Institutes of Advanced Technology, Xiong, Zhiqiang; Institute of Applied Ecology Chinese Academy of Sciences Ma, Wei; Nankai University Wang, Dongsheng; Institute of Applied Ecology Chinese Academy of Sciences Zhang, Xuejiao; Institute of Applied Ecology, CAS, ; Xing, Baoshan; UMASS, Stockbridge School of Agriculture

Environmental significance

The access to pathogen-free drinking water is urgently needed for billions of people worldwide. However, the traditional water disinfection techniques have limitations in tedious operation, high energy consumption, membrane fouling, and environmental and health risks. Herein, we fabricated a sandwich-structured filter system (CSBPP) by layer-by-layer sequential stacking of chitosan hydrogel, black phosphorus (BP), and chitosan hydrogel for NIR-triggered water disinfection. The bacterial cells could be captured by the chitosan hydrogel via pore interception and electrostatic adsorption. Meanwhile, the adhered bacteria underwent completely sterilization (> 140 ^{o}C) due to the superior photothermal property of BP nanosheets, which could solve the issue of membrane fouling. Apart from the commonly used *B. subtilis* and *E. coli*, CSBPP was also feasible for inactivating antibiotic resistant bacteria and removal multiple microorganisms from natural water.

ARTICLE

Filtration-based water treatment system embedded with black phosphorus for NIR-triggered disinfection

Dengyu Li [a, c, †], Qing Zhao [a, †], Siyu Zhang [a, b], Fengchang Wu [d], Xuefeng Yu [e], Zhiqiang Xiong [a, c], Wei Ma [a, c], Dongsheng Wang [a, c], Xuejiao Zhang [a, *], Baoshan Xing [b]

[a] Key Laboratory of Pollution Ecology and Environmental Engineering, Institute of Applied Ecology, Chinese Academy of Sciences, Shenyang 110016, China.

[b] Stockbridge School of Agriculture, University of Massachusetts, Amherst, MA 01003, USA

[c] University of Chinese Academy of Sciences, Beijing 100049, China

[d] State Key Laboratory Environmental Criteria and Risk Assessment, Chinese Research Academy of Environmental Sciences, Beijing 100012, China

[e] Center for Biomedical Materials and Interfaces Shenzhen Institutes of Advanced Technology, Chinese Academy of Sciences, Shenzhen 518055, P. R. China

† These authors contributed equally.

*Corresponding author

Dr. Xuejiao Zhang; E-mail: zhangxuejiao@iae.ac.cn

Abstract

Facile, efficient, and safe techniques for water disinfection are urgently needed, especially for people who cannot access pathogen-free drinking water. Here, a sandwich-structured filter system (CSBPP) is designed and constructed by layer-by-layer sequential stacking in the order of chitosan hydrogel, black phosphorus (BP) nanosheets, and chitosan hydrogel for near-infrared (NIR)-triggered point-of-use (POU) water disinfection. Above 99% of bacterial cells can be captured by CSBPP during filtration, which is attributed to the pore interception and electrostatic adsorption by the chitosan hydrogel. Almost 100% of entrapped bacterial cells can be inactivated under 808 nm illumination due to the photothermal bactericidal function of BP nanosheets, which can suppress the membrane fouling induced by the undesirable growth of bacteria. The operation is convenient, with no need for high energy-input, which is superior to cryogels and conventional filtration membranes. The BP nanosheets can also improve the safety by avoiding the release of toxic metal ions that occurs in the conventional POU water disinfection systems. Notably, the removal-disinfection process can be repeated at least 10 times without compromising the effectiveness. Thus, the CSBPP has great potential as an alternative POU approach for potent, practical, and safe water disinfection.

ARTICLE

1. Introduction

Currently, at least 1.8 billion people worldwide are under threat of the pathogen-contaminated drinking water.[1-3] Waterborne pathogens cause several million deaths and numberless cases of sickness every year. Moreover, the abuse of antibiotics has led to the issue of antimicrobial resistance (AMR), and drinking water is regarded as a potential route of AMR spreading to humans due to horizontal gene transfer.[4-6] Traditional water disinfection techniques, such as chlorination and ozonation, are not effective in controlling AMR spread. Additionally, disinfectant agents are generally toxic themselves and can produce byproducts that are harmful to human health.[7, 8] Moreover, in some resource-limited developing countries or under emergency situations (e.g., after natural disasters), centralized water disinfection infrastructures are scarce. The World Health Organization (WHO) suggests that point-of-use (POU) water treatment is a promising solution for low-quality household drinking water.[9] In addition, several meta-analyses reported that POU techniques are more effective in improving water quality at the household level than are interventions at the water source.[9-11] Thus, facile, efficient, and safe POU water disinfection techniques have gained increasing attention and interest.

Recently, cryogels have been applied for POU water disinfection.[1, 8, 12] These gels normally possess large pore sizes of a few to hundreds of micrometers, excellent mechanical properties, and superior water absorption ability. However, this

purification process is tedious and only suitable for small-scale water disinfection since the swollen cryogels must be squeezed to recover the absorbed water. In addition to cryogels, filtration membranes, with pore sizes generally smaller than the size of microorganisms, have been used for POU bacterial removal by the size-exclusion effect.[13-16] Although filtration membranes offer a simpler process and produce larger amounts of disinfected water than cryogels, they always require vacuum or pressure due to their small pore size, which is not practical for potable water disinfection. Another issue restricting the widespread application of membrane technology is membrane fouling due to the undesirable growth of microorganisms on the membrane surface, which can block the membrane pores and hinder the water flux. In these water disinfection systems, silver nanoparticles (NPs),[1, 17, 18] copper NPs,[19, 20] $La(OH)_3$ nanorods[21-23] and graphene/metal composite nanomaterials[1, 8, 24, 25] have been employed as bactericidal agents. Despite their outstanding bactericidal capabilities, these materials are limited in practical applications because toxic metal ions can be accidentally leaked during long-term use, which is potentially hazardous to ecological, environmental and human health.[26-28]

It has been proven that light-triggered photo-to-thermal conversion is effective for water disinfection using photothermal agents (e.g., carbon black, gold nanorods, Prussian blue nanocages, and Cs0.33WO3).[29-31] In these studies, photothermal nanobactericides were either in the suspension state or attached onto the inner surfaces of microchannels. However, free-state NPs are difficult to recycle from disinfected water, and particles on microchannel surfaces are mobile due to the lack of constraints. Therefore, it is essential to build a novel water disinfection system that can solve all

these problems, including tedious operation, high energy consumption, membrane fouling, and environmental and health risks.

Black phosphorus (BP) is a newly emerging two-dimensional nanomaterial which has shown great potential in electronics, photonics, theranostics, and catalysis due to its unique features.[32-36] In particular, BP nanosheets efficiently convert near-infrared (NIR) light into thermal energy, which has the capacity for use in photothermal cancer therapy.[37-39] Very recently, BP nanosheets have been proposed to be excellent bactericides under NIR irradiation and exhibited excellent antibacterial effects during postsurgery healing.[40] Recently, with the rapid development of BP's manufacture technique, its production cost has been less than $1 per gram,[41-43] which provides a solid foundation for the large-scale applications of BP, including water treatment. These facts suggest the potential of BP nanosheets as outstanding nanobactericides for the fabrication of POU water disinfection systems, which has, however, still been uncovered until now.

Herein, we fabricated a sandwich-structured POU water disinfection system (CSBPP) based on layer-by-layer sequential stacking in the order of chitosan hydrogel, BP nanosheets, and chitosan hydrogel (Scheme 1). The chitosan hydrogel networks are devoted to bacterial capture through electrostatic interactions between the positively charged chitosan and the negatively charged bacterial wall.[44, 45] At the same time, the embedded BP nanosheets contribute to disinfection via photo-to-thermal conversion under NIR illumination.[32] The potency was maintained even after ten cycles of performance, indicating that CSBPP will be a promising candidate for powerful and practical POU water disinfection.

2. Materials and methods

2.1 Materials

Chitosan (85% deacetylated) was obtained from Aladdin Reagent Co., Ltd. (Shanghai, China). BP crystals (99.98%) were bought from Mophos (Mophos.cn, China). The acridine orange/ethidium bromide (AO/EB) assay kit was obtained from Solarbio Science & Technology Co., Ltd. (Beijing, China). Cellulose filter paper (F-paper, mesh size 20 μm) was obtained from Hangzhou Whatman-Xinhua Filter Paper Co., Ltd. (Hangzhou, China). Glutaraldehyde aqueous solution (50 wt%) and sodium borohydride (NaBH4) were purchased from Damao Reagent Co., Ltd. (Tianjin China). All other materials were of analytical grade and used as received. *Escherichia coli* (*E. coli*), *Bacillus subtilis* (*B. subtilis*), and ampicillin-resistant *E. coli* (re-Amp. *E. coli*) were provided by Heilongjiang Provincial Key Laboratory of Environmental Microbiology and Recycling of Argo-Waste in Cold Region (Daqing, China).

2.2 Preparation of chitosan-coated F-Paper (CSP)

The F-paper was wrapped with chitosan hydrogel by crosslinking with glutaraldehyde via a Schiff base reaction. Briefly, F-paper with a diameter of 5.5 cm was immersed in 1.0 wt% chitosan solution (10 mL) at room temperature for 1 h, allowing the F-paper to be thoroughly covered with chitosan molecules. Then, it was immersed in 10 mL of glutaraldehyde solution (2.5, 5, 10, 15, and 20 wt%) for 10 h. After being rinsed with deionized (DI) water several times, the papers were immersed in $NaBH_4$ solution (0.5 g mL^{-1}) overnight at room temperature. Finally, the obtained CSP was thoroughly washed with DI water and dried overnight at room temperature before use.

2.3 Preparation of BP nanosheets-embedded CSP (CSBPP)

The CSP was cut into round discs with diameters of 14 mm and fixed into a sterile syringe filter. A suspension of BP nanosheets (500 μg mL^{-1}) was filtrated through the syringe filter for 5 times to adequately load the BP nanosheets onto the CSP. Then, the BP-coated CSP was equipped with another layer of chitosan hydrogel following the same procedure as that used for CSP preparation, producing the sandwich-structured CSBPP.

2.4 Characterizations

The morphologies were monitored using a transmission electron microscope (TEM, JEOL 2100) operated at an accelerating voltage of 200 kV. Atomic force microscopy (AFM, Agilent 5100) was used to characterize the thickness and lateral size of the BP nanosheets in tapping mode. The chemical compositions of the BP nanosheets were detected by X-ray photoelectron spectroscopy (XPS, ESCALAB250, Thermo VG) using a monochromated A1 Kα X-ray source at 1486.6 eV. The concentration of the BP nanosheets was determined by inductively coupled plasma-optical emission spectrometry (ICP-OES). The surface morphologies of various papers and bacterial samples were examined by scanning electron microscopy (SEM, Hitachi S-4700 or FEI Quanta 250). The elemental distributions of the paper samples were obtained using an FEI Quanta 250 SEM equipped with an energy-dispersive X-ray analysis system (SEM-EDX, Ametek, USA). The hydrodynamic size of the BP nanosheets was determined by a Zetasizer Nano ZS (Malvern Instruments) equipped with a 633 nm He–Ne laser at 25 °C. Fourier-transform infrared (FTIR) spectra were obtained using a FTIR spectrometer (Nicolet 6700, Thermo Fisher Scientific, USA).

2.5 Bacterial filtration

The bacterial removal efficiencies of the F-paper, CSP, and CSBPP were tested against two model bacterial strains, gram-negative *E. coli* and gram-positive *B. subtilis*. Both bacterial strains were cultured in beef extract peptone medium (containing 10 g bacto-tryptone, 5 g beef extract, and 5 g NaCl in 1 L of water) at 37 °C and harvested in the mid-exponential growth phase. The F-paper, CSP, and CSBPP (diameter = 14 mm) were fixed into the sterile syringe filters. Both *E. coli* and *B. subtilis* stock suspensions were diluted to a final concentration of ~3×10^5 colony forming units (CFU) per mL with sterilized water before use. Then, 1 mL of the bacterial suspensions was filtered through a syringe by gravity at a flow rate of 0.2 mL min^{-1}. To test the reusability, the CSBPP was sonicated for 10 min and thoroughly washed with sterile water after filtration.[26] Next, the filtration process was repeated a predetermined number of times. The filtrates were serially diluted (10^{-1}, 10^{-2}, 10^{-3}) with sterilized water, and 100 μL of each dilution was sprayed onto the nutrition agar plates. The bacterial colonies were recorded after 24 h incubation at 37 °C. For the natural water filtration test, different volumes (20, 40, and 60 mL) of water from Hun River (Liaoning Province, China) were filtrated through the CSBPP. Then, the DNA concentrations in the filtrates were determined by fluorescent quantitative polymerase chain reaction (qPCR) according to the reported procedure[46]. All experiments were repeated three times.

2.6 Photothermal-triggered bactericidal activity

The bactericidal activity of the CSBPP under NIR illumination was studied by the colony counting method, SEM, and fluorescence assay. The F-paper, CSP, and CSBPP (diameter = 14 mm) were respectively covered with a same-sized sterilized membrane (pore size = 0.22 μm) with a hole (diameter = 5 mm) in the middle and equipped in the syringe filter. After filtration, bacterial cells were attached to the bare space of the paper samples, which was

illuminated with NIR light at 808 nm. Then, the paper samples were sonicated in 1 mL sterilized water for 7 min to detach the bacteria according to a previously reported protocol,[24, 47, 48] followed by quantification of the bacterial density by plate counting method as described above. The control group (pristine bacterial suspension) also experienced sonication for the same time period to eliminate the interference of sonication step. To verify the reusability, the CSBPP was thoroughly rinsed with DI water to remove the bacterial debris after one round of testing, and the process was repeated a predetermined number of times.

2.7 Fluorescence assay

The photothermal-induced bactericidal effect was visualized by AO/EB double staining. In brief, the bacterial cells were detached from the paper samples following the above procedure and were stained with an AO/EB staining kit for 10 min. Then, the bacterial pellets were centrifuged at 8000 rpm for 5 min and rinsed with PBS. Afterwards, the specimens were dropped onto microscope slides, covered with cover slips, and visualized by inverted fluorescence microscopy (Leica, DMI3000B, Germany).

2.8 Morphology observation by SEM

The morphologies of the bacterial cells on the CSBPP with/without illumination were observed by SEM. After filtration, the paper samples were fixed with 2.5% glutaraldehyde for 3 h and consecutively dehydrated with a series of concentrations of ethanol aqueous solutions (50, 70, 90, and 100%) individually for 10 min. Afterwards, the coupons were sequentially immersed in tert-butyl alcohol (50% and 100%) for 20 min, followed by lyophilization. The samples were imaged by SEM operating at an acceleration voltage of 5-10 kV.

3. Results and discussions

3.1 Exfoliation and characterization of BP nanosheets

BP nanosheets were prepared by liquid-phase exfoliation of the BP crystals in oxygen-free Millipore water using a facile tip sonication process followed by centrifugation at 1000 rpm to remove the bulk BP.[49] The prepared BP nanosheets were well-dispersed and exhibited a regular lamellar structure (Figure S1A, B). Their average thickness and lateral size were 5.1 ± 2.6 nm and 116.8 ± 43.9 nm, respectively, according to statistical analysis of the AFM images (Figure S1C, D). The BP nanosheets had a broad light absorbance across the UV, visible, and NIR light regions, endowing BP the ability not only to generate reactive oxygen species (ROS) as an efficient photosensitizer but also to convert NIR light into thermal energy (Figure S1E).[39, 50] The characteristic peak of crystalline BP at 127.1 eV and a small peak at 131 eV, assigned to the oxidized phosphorus, were observed in the XPS spectrum (Figure S1F).[51-53]

3.2 Fabrication and characterizations of CSBPP

The POU water disinfection membrane, namely, the CSBPP, was constructed by a sandwich-producing approach. First, the F-paper (Figure 1A,D) was coated with chitosan hydrogel formed by the crosslinking of chitosan with glutaraldehyde via a Schiff base reaction to produce CSP (Figure 1B). Compared to the bare F-paper, an increased roughness of the cellulose fibers in CSP was observed (Figure 1E). Moreover, the FTIR spectrum (Figure S2) of the CSP showed the stretching vibration bands of $–CH_3$ (2920 cm^{-1}) and amide (1558 and 1647 cm^{-1}).[54] These results indicated the F-paper was covered with chitosan hydrogel, which facilitates the loading of BP nanosheets. To stabilize the loaded BP nanosheets, a second

layer of chitosan hydrogel was deposited on top of the BP layer, forming a sandwich-like structure on the F-paper (Figure 1C). The emergence of numerous granules on the fibers of CSBPP (Figure 1F), the characteristic peaks of BP at 2050 and 2180 cm^{-1} in the FTIR spectrum of CSBPP (Figure S2), together with the energy-dispersive X-ray (EDX) mapping images (Figure S3, Table S1), verified the successful loading of BP nanosheets on the CSBPP. Four CSBPPs containing different amounts of BP nanosheets (CSBPP1: 24 μg cm^{-2}, CSBPP 2: 49 μg cm^{-2}, CSBPP 3: 123 μg cm^{-2}, CSBPP 4: 247 μg cm^{-2}) were obtained.

3.3 Bacterial removal by the sandwich-structured water disinfection system

The bacteria-containing water was filtered through the paper samples via a syringe, which is more easily operable than the traditional membrane technique that requires a pump. The bacterial removal efficiency was quantified by the colony counting method. Apparently, the removal efficiency was related to the pore size of the chitosan hydrogels and the amount of residual amino groups following crosslinking, both of which were determined by the crosslinking degree—in other words, the crosslinker concentration. Thus, CSPs (CSP2.5, CSP5, CSP10, CSP15, and CSP20) crosslinked with different glutaraldehyde concentrations (2.5, 5, 10, 15, and 20%) were fabricated. As the glutaraldehyde concentration increased from 2.5% to 20%, the bacterial removal efficiency first increased and then decreased, with a maximum value of ~ 98% for CSP10 (Figure 2A), which indicated an optimal combination of the pore size and amine amount was acquired. The pores of the chitosan hydrogel were too large to intercept the bacterial cells at lower glutaraldehyde concentrations (< 10%), whereas the amino residues in the hydrogel were inadequate to interact with the bacterial cells if excess glutaraldehyde (> 10%) was used. Thus, the CSP crosslinked with 10% glutaraldehyde was used to load the BP nanosheets in the following studies.

3.4 Photothermal bactericidal effect

It is known that BP nanosheets have considerable photothermal efficiency under NIR irradiation,[50] endowing the CSBPP with the possible capacity to kill bacterial cells absorbed onto the hydrogel scaffold via a photothermal effect. The photothermal bactericidal performances of CSBPPs (1-4) were evaluated against *E. coli* under the illumination with an NIR light (808 nm, 0.5 W cm^{-2}) for 30 min. In the meantime, the paper temperature was monitored by a thermal camera (FLIR E4) as a function of the illumination time.

The temperature followed a two-stage rising profile during the 30-min NIR illumination (Figure 2B). In the first stage, the temperature increased by 20-30 °C within 1 min and exhibited a plateau period for 5-11 min for the CSBPPs (1-4), during which the heat energy generated by the BP nanosheets was consumed to evaporate the surface water. Afterwards, a second stage of the temperature rise was observed, with final equilibrium temperatures of 101, 115, 128, and 144 °C for the CSBPPs (1, 2, 3 and 4, respectively). The heating rate and vertex temperature depended on the loading content of BP nanosheets. After illumination, the heat map of CSBPP4 exhibited a maximum temperature above 140 °C in the central region of the light spot (Figure 2C). The temperature was sufficient to denature the enzymes and proteins in bacterial cells and to damage the lipid membrane, eventually leading to bacterial inactivation.[55] Compared to the F-paper and CSP, the bactericidal efficiencies of the CSBPPs were significantly enhanced (Figure 2D). Specifically, as the loading of BP nanosheets was elevated from 24 to 247 μg cm^{-2}, the bactericidal efficiency increased from 34% to 99.99%, which was accompanied by a positive correlation with the temperature rise trend. Thus, CSBPP4, simplified as CSBPP, was the most potent and was applied in the following studies.

3.5 Integration efficiency of bacterial removal and disinfection for CSBPP

After optimizing the composition, we monitored the performance of CSBPP in POU water disinfection. The bacterial removal efficiencies of F-paper toward both gram-positive *B. subtilis* and gram-negative *E. coli* were significantly enhanced from 76% and 40% to ~98% by coating with chitosan hydrogel (Figure 3A), indicating efficient capture of bacterial cells by the chitosan hydrogel. The removal capacity of CSBPP was in parallel with that of CSP, with efficiencies of 98.1% and 98.5% for *B. subtilis* and *E. coli* (Figure 3A,C), which can be further raised to 99.15% and 99.99%, respectively, by filtration twice (Figure S4). More importantly, CSBPP maintained a high removal efficiency (> 98%) against *E. coli* even after 15 cycles (Figure S5), demonstrating its reusability. To verify the applicability of CSBPP for purifying natural water, the DNA concentration determined by qPCR was used to quantify the number of microorganisms in the natural water before and after filtration (Figure S6). The removal efficiency was unexpectedly increased upon enhancing the throughput. This result might be attributed to the chitosan hydrogel becoming denser and the pores becoming more or less blocked during the adsorption of microorganisms, thus resulting in the enhanced interception capacity of CSBPP.

Then, we tested the bactericidal effect of CSBPP after bacterial filtration under NIR light illumination (Figure 3B,D). For the F-paper and CSP, no bactericidal effect was detected with or without NIR treatment. In contrast, no visible colony in CSBPP was visualized for either bacterial strain in agar plates after exposure to NIR illumination, demonstrating that the photothermal performance of the embedded BP nanosheets was sufficient to sterilize almost 100% of the bacteria (Figure 3B,D). Specifically, the bactericidal efficiency remained steady (> 99.9%) even after 10 cycles of operation (Figure S7). More importantly, CSBPP was also effective in disinfection of the antibiotic-resistant strain, re-Amp. *E. coli* (Figure S8). Thus,

membrane fouling could be circumvented due to complete inactivation of the attached bacterial cells by BP's photothermal effect under NIR light illumination.

To further confirm the effectiveness of CSBPP for POU water disinfection, AO/EB staining was performed to visualize the bacterial viability after bactericidal treatment (Figure 4A). Both *B. subtilis* and *E. coli* emitted green fluorescence but no red fluorescence without NIR illumination, demonstrating that the bacterial cells remained alive with intact membranes after only contacting CSBPP. Upon exposure to NIR light, nearly all bacterial cells showed red fluorescence, which represented dead cells with membranes permeable to EB. In addition, the changes in membrane integrity and morphology were evaluated by SEM (Figure 4B). In the absence of NIR light, the bacterial cells adhered onto CSBPP had regular rod shapes with smooth surfaces and intact structures. After NIR illumination, the morphology of the bacterial cells for both strains was significantly altered, with apparent shape distortion, loss of membrane integrity, and production of cell debris.

3. Conclusions

A filter paper-based POU water disinfection system (CSBPP) was successfully developed by a facile sandwich-making process, employing BP nanosheets as a new photothermal nanobactericide for water disinfection. Owing to its high hydrophilicity, CSBPP allowed water to easily pass through in the absence of a vacuum pump, and the bacterial cells were harvested by the chitosan hydrogel via both pore interception and electrostatic interactions. Then, the bacteria on CSBPP underwent complete high-temperature sterilization (> 140 °C) due to the superior photothermal properties of the BP nanosheets, which circumvented membrane fouling and endowed CSBPP with a steady high efficiency in bacterial removal and disinfection (> 10 cycles). Apart from the commonly used *B. subtilis* and *E. coli*, CSBPP

was also feasible for inactivating antibiotic-resistant bacteria and for the removal of multiple microorganisms from natural water. Considering the biodegradability of BP nanosheets, CSBPP was more environmentally benign than heavy metal-containing water disinfection systems and, thus, has great potential for potent, practical, and safe water disinfection. Furthermore, BP nanosheets, as a new photothermal nanobactericide, may also find use in antibiofouling and anti-infection therapy.

Conflicts of interest

The authors declare no competing financial interest.

Acknowledgements

Q. Z. and D. L. contributed equally to this paper. This work was supported by the National Natural Science Foundation of China (No. 41877389, 41603120, 41703107, and 21607165), the National Key Research and Development Program of China (No. 2016YFD0800300), the Youth Innovation Promotion Association CAS awarded to S.-Y.Z. (2017-2020), the Open Foundation of State Key Laboratory of Environmental Criteria and Risk Assessment, the Chinese Research Academy of Environmental Sciences (sklecra OFP 2016), the Hundreds Talents Program of the Chinese Academy of Sciences awarded to X.-J.Z. (2015-2020) and Q.Z. (2014-2019), and the USDA-NIFA Hatch Program (MAS 00475).

References

1. S.-L. Loo, W. B. Krantz, A. G. Fane, Y. Gao, T.-T. Lim and X. Hu, *Environ. Sci. Technol.*, 2015, **49**, 2310-2318.

2. R. P. Schwarzenbach, B. I. Escher, K. Fenner, T. B. Hofstetter, C. A. Johnson, U. von Gunten and B. Wehrli, *Science*, 2006, **313**, 1072-1077.
3. Y. L. F. Musico, C. M. Santos, M. L. P. Dalida and D. F. Rodrigues, *ACS Sustainable Chem. Eng.*, 2014, **2**, 1559-1565.
4. T. Schwartz, W. Kohnen, B. Jansen and U. Obst, *FEMS Microbiol. Ecol.*, 2003, **43**, 325-335.
5. A. Pruden, R. Pei, H. Storteboom and K. H. Carlson, *Environ. Sci. Technol.*, 2006, **40**, 7445-7450.
6. C. Xi, Y. Zhang, C. F. Marrs, W. Ye, C. Simon, B. Foxman and J. Nriagu, *Appl. Environ. Microbiol.*, 2009, **75**, 5714-5718.
7. Y. I. Seo, K. H. Hong, S. H. Kim, D. Chang, K. H. Lee and Y. D. Kim, *J. Hazard. Mater.*, 2012, **s 227–228**, 469-473.
8. S. L. Loo, A. G. Fane, T. T. Lim, W. B. Krantz, Y. N. Liang, X. Liu and X. Hu, *Environ. Sci. Technol.*, 2013, **47**, 9363-9371.
9. T. F. Clasen, K. T. Alexander, S. David, B. Sophie, P. Rachel, H. H. Chang, M. Fiona and C. Sandy, *Cochrane Database Syst. Rev.*, 2015, **334**, 1-201.
10. L. Fewtrell, R. B. Kaufmann, D. Kay, W. Enanoria, L. Haller and J. M. Colford, *Lancet Infect. Dis.*, 2005, **5**, 42-52.
11. J. S. Gruber, A. Ercumen and J. M. C. Jr, *PLoS ONE*, 2014, **9**, e107429.
12. S. J. Shirbin, J. L. Shu, J. A. Chan, M. M. Ozmen, Q. Fu, N. O'Briensimpson, E. C. Reynolds and G. G. Qiao, *ACS Macro Lett.*, 2016, **5**, 552-557.
13. S. Y. Yang, I. Ryu, H. Y. Kim, J. K. Kim, S. K. Jang and T. P. Russell, *Adv. Mater.*, 2010, **18**, 709-712.
14. P. Gunawan, C. Guan, X. Song, Q. Zhang, S. S. Leong, C. Tang, Y. Chen, M. B. Chanpark, M. W. Chang and K. Wang, *ACS Nano*, 2011, **5**, 10033-10040.
15. H. Ma, C. Burger, B. S. Hsiao and B. Chu, *Biomacromolecules*, 2011, **12**, 970-976.
16. B. P. Nellore, R. Kanchanapally, F. Pedraza, S. S. Sinha, A. Pramanik, A. T. Hamme, Z. Arslan, D. Sardar and P. C. Ray, *ACS Appl. Mater. Interfaces*, 2015, **7**, 19210.
17. T. A. Dankovich and D. G. Gray, *Environ. Sci. Technol.*, 2011, **45**, 1992-1998.
18. X. Zeng, D. T. Mccarthy, A. Deletic and X. Zhang, *Adv. Funct. Mater.*, 2015, **25**, 4344-4351.
19. T. A. Dankovich and J. A. Smith, *Water Res.*, 2014, **63**, 245-251.
20. T. A. Dankovich, J. S. Levine, N. Potgieter, R. Dillingham and J. A. Smith, *Environ. Sci.: Water Res. Technol.*, 2016, **1**, 85.
21. J. He, W. Wang, F. Sun, W. Shi, D. Qi, K. Wang, R. Shi, F. Cui, C. Wang and X. Chen, *ACS Nano*, 2015, **9**, 9292-9302.
22. J. He, W. Wang, R. Shi, W. Zhang, X. Yang, W. Shi and F. Cui, *Chem. Eng. J.*, 2018, **337**, 428-435.
23. X. Zhang, W. Wang, W. Shi, J. He, H. Feng, Y. Xu, F. Cui and C. Wang, *Journal of Materials Chemistry A*, 2016, **4**, 12799-12806.
24. Y. Jiang, W. N. Wang, D. Liu, Y. Nie, W. Li, J. Wu, F. Zhang, P. Biswas and J. D. Fortner, *Environ. Sci. Technol.*, 2015, **49**, 6846.
25. X. Xie, C. Mao, X. Liu, Y. Zhang, Z. Cui, X. Yang, Y. Kwk, H. Pan, P. K. Chu and S. Wu, *ACS Appl. Mater. Interfaces*, 2017, **9**.
26. R. K. Shukla, A. Kumar, D. Gurbani, A. K. Pandey, S. Singh and A. Dhawan, *Nanotoxicology*, 2013, **7**, 48-60.
27. P. Chairuangkitti, S. Lawanprasert, S. Roytrakul, S. Aueviriyavit, D. Phummiratch, K. Kulthong, P. Chanvorachote and R. Maniratanachote, *Toxicology in Vitro An International Journal Published in Association with Bibra*, 2013, **27**, 330-338.

28. M. I. Setyawati, X. Yuan, J. Xie and D. T. Leong, *Biomaterials*, 2014, **35**, 6707-6715.
29. T. Jiang, J. He, L. Sun, Y. Wang, Z. Li, Q. Wang, Y. Sun, W. Wang and M. Yu, *Environmental Science: Nano*, 2018, **5**, 1161-1168.
30. Y. K. Kim, E. B. Kang, S. M. Kim, C. P. Park, I. In and S. Y. Park, *ACS Appl. Mater. Interfaces*, 2017, **9**, 3192-3200.
31. S. Loeb, C. Li and J.-H. Kim, *Environ. Sci. Technol.*, 2018, **52**, 205-213.
32. J. Shao, C. Ruan, H. Xie, Z. Li, H. Wang, P. K. Chu and X. F. Yu, *Adv. Sci.*, 2018, **5**, 1700848.
33. L. Li, Y. Yu, G. J. Ye, Q. Ge, X. Ou, H. Wu, D. Feng, X. H. Chen and Y. Zhang, *Nat. Nanotechnol.*, 2014, **9**, 372-377.
34. X. Wang, A. M. Jones, K. L. Seyler, V. Tran, Y. Jia, H. Zhao, H. Wang, L. Yang, X. Xu and F. Xia, *Nat. Nanotechnol.*, 2015, **10**, 517-521.
35. M. Qiu, D. Wang, W. Liang, L. Liu, Y. Zhang, X. Chen, D. K. Sang, C. Xing, Z. Li and B. Dong, *Proc. Natl. Acad. Sci. U. S. A.*, 2018, **115**, 501.
36. N. M. Latiff, W. Z. Teo, Z. Sofer, A. C. Fisher and M. Pumera, *Chem. Eur. J.*, 2015, **21**, 14232-14232.
37. C. Sun, L. Wen, J. Zeng, Y. Wang, Q. Sun, L. Deng, C. Zhao and Z. Li, *Biomaterials*, 2016, **91**, 81-89.
38. J. Shao, H. Xie, H. Huang, Z. Li, Z. Sun, Y. Xu, Q. Xiao, X. F. Yu, Y. Zhao and H. Zhang, *Nat. Commun.*, 2016, **7**, 12967.
39. Z. Sun, H. Xie, S. Tang, X. Yu, Z. Guo, J. Shao, H. Zhang, H. Huang, H. Wang and P. Chu, *Angew. Chem., Int. Ed.*, 2015, **127**, 11526-11530.
40. Z. Sun, Y. Zhang, H. Yu, C. Yan, Y. Liu, S. Hong, H. Tao, A. W. Robertson, Z. Wang and A. A. H. Pádua, *Nanoscale*, 2018, **10**, 12543-12553.
41. M. Wen, J. Wang, R. Tong, D. Liu, H. Huang, Y. Yu, Z.-K. Zhou, P. K. Chu and X.-F. Yu, *Adv. Sci.*, 2019, **6**, 1801321.
42. Y. Zhao, T. L. Chen, L. Xiao, M. A. Kolaczkowski, L. Zhang, L. M. Klivansky, V. Altoe, B. Tian, J. Guo, X. Peng, Y. Tian and Y. Liu, *Nano Energy*, 2018, **53**, 345-353.
43. T. G. Novak, H. Shin, J. Kim, K. Kim, A. Azam, C. V. Nguyen, S. H. Park, J. Y. Song and S. Jeon, *ACS Appl. Mater. Interfaces*, 2018, **10**, 17957-17962.
44. D. Raafat, B. K. Von, A. Haas and H. G. Sahl, *Appl. Environ. Microbiol.*, 2008, **74**, 3764.
45. I. M. Helander, E. L. Nurmiaho-Lassila, R. Ahvenainen, J. Rhoades and S. Roller, *Int. J. Food Microbiol.*, 2001, **71**, 235-244.
46. H. Zhu, F. Qu, Zhu and L. H, *Nucleic Acids Res.*, 1993, **21**, 5279-5280.
47. F. Perreault, M. E. Tousley and M. Elimelech, *Environ. Sci. Technol. Lett.*, 2014, **1**, 71-76.
48. M. S. Mauter, Y. Wang, K. C. Okemgbo, C. O. Osuji, E. P. Giannelis and M. Elimelech, *ACS Appl. Mater. Interfaces*, 2011, **3**, 2861-2868.
49. X. Zhang, Z. Zhang, S. Zhang, D. Li, W. Ma, C. Ma, F. Wu, Q. Zhao, Q. Yan and B. Xing, *Small*, 2017, **13**, 1701210.
50. Y. Zhao, H. Wang, H. Huang, Q. Xiao, Y. Xu, Z. Guo, H. Xie, J. Shao, Z. Sun, W. Han, X.-F. Yu, P. Li and P. K. Chu, *Angew. Chem., Int. Ed.*, 2016, **55**, 5003-5007.
51. J. D. Wood, S. A. Wells, D. Jariwala, K.-S. Chen, E. Cho, V. K. Sangwan, X. Liu, L. J. Lauhon, T. J. Marks and M. C. Hersam, *Nano Lett.*, 2014, **14**, 6964-6970.
52. J. Kang, J. D. Wood, S. A. Wells, J.-H. Lee, X. Liu, K.-S. Chen and M. C. Hersam, *ACS Nano*, 2015, **9**, 3596-3604.
53. P. Yasaei, B. Kumar, T. Foroozan, C. Wang, M. Asadi, D. Tuschel, J. E. Indacochea, R. F. Klie and A. Salehi-Khojin, *Adv. Mater.*, 2015, **27**, 1887-1892.

54. B. Li, C. L. Shan, Q. Zhou, Y. Fang, Y. L. Wang, F. Xu, L. R. Han, M. Ibrahim, L. B. Guo and G. L. Xie, *Mar. Drugs*, 2013, **11**, 1534-1552.
55. C. W. Hsiao, H. L. Chen, Z. X. Liao, R. Sureshbabu, H. C. Hsiao, S. J. Lin, Y. Chang and H. W. Sung, *Adv. Funct. Mater.*, 2015, **25**, 721–728.

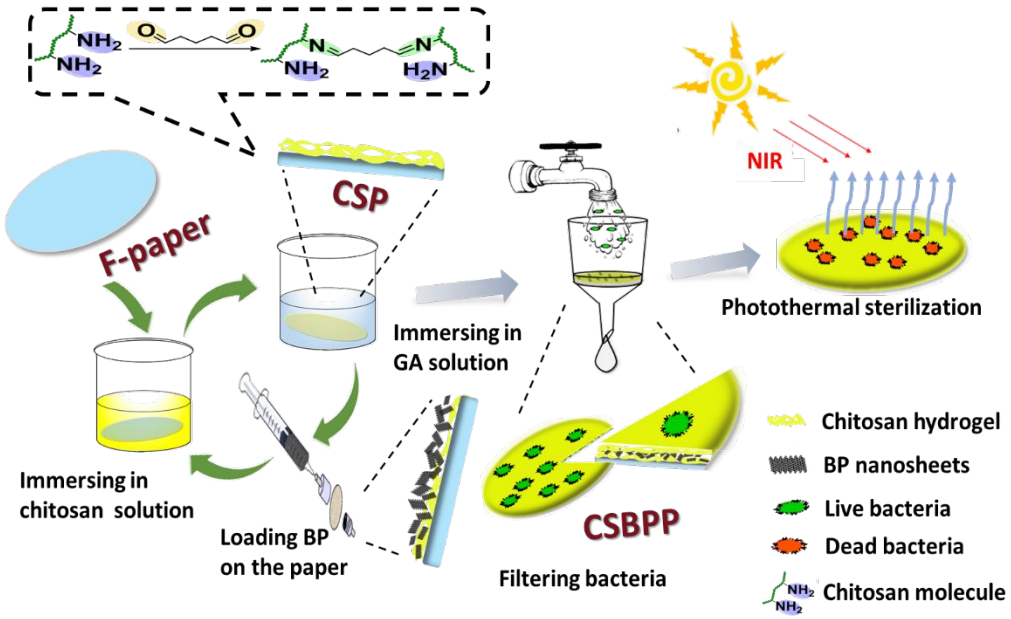

Scheme 1. Fabrication process of the sandwich-structured filter systems and the description of bacteria removal-disinfection.

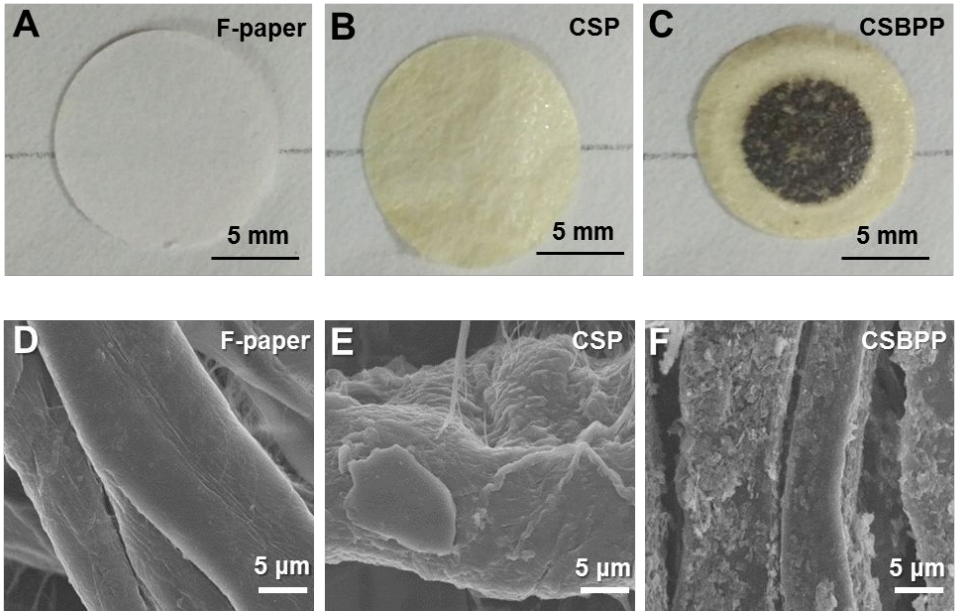

Figure 1. Photographs (A, B, C) and SEM images (D, E, F) of the F-paper, CSP, and CSBPP.

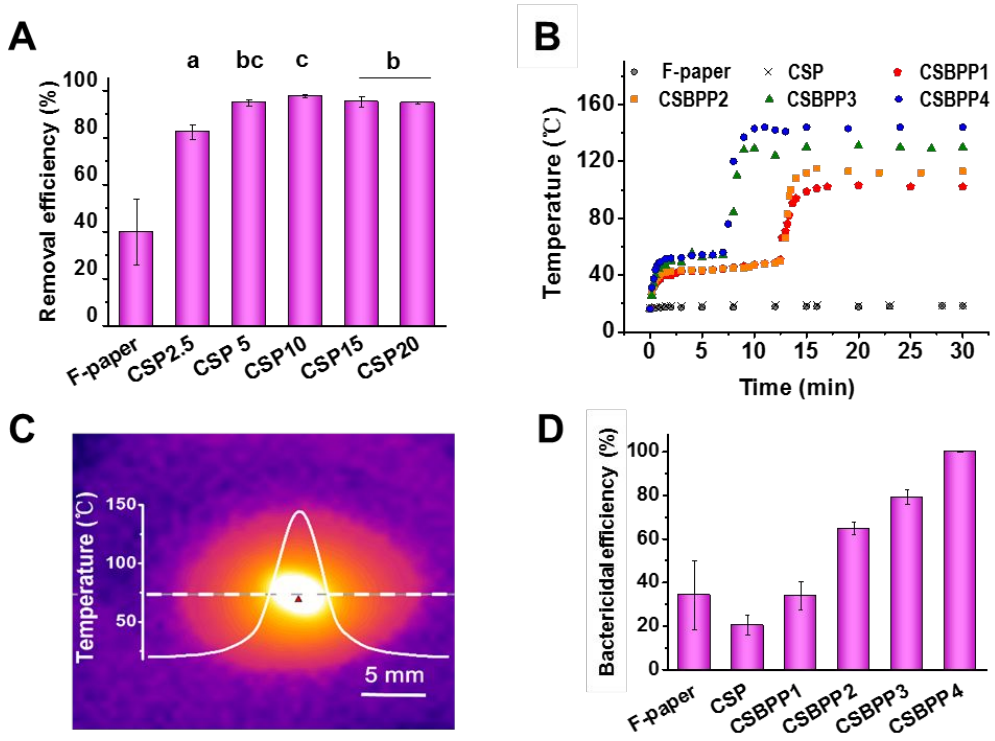

Figure 2. (A) Removal efficiency for *E. coli* treated by F-paper and CSP with different crosslinking degrees. (B) Temperature evolution curves of various F-papers over time under exposure to NIR light. (C) Thermographic image of CSBPP4 after 10 min of NIR illumination. (D) Bactericidal efficiency toward *E. coli* treated by the F-paper, CSP, and CSBPPs (1-4) post-NIR illumination for 30 min.

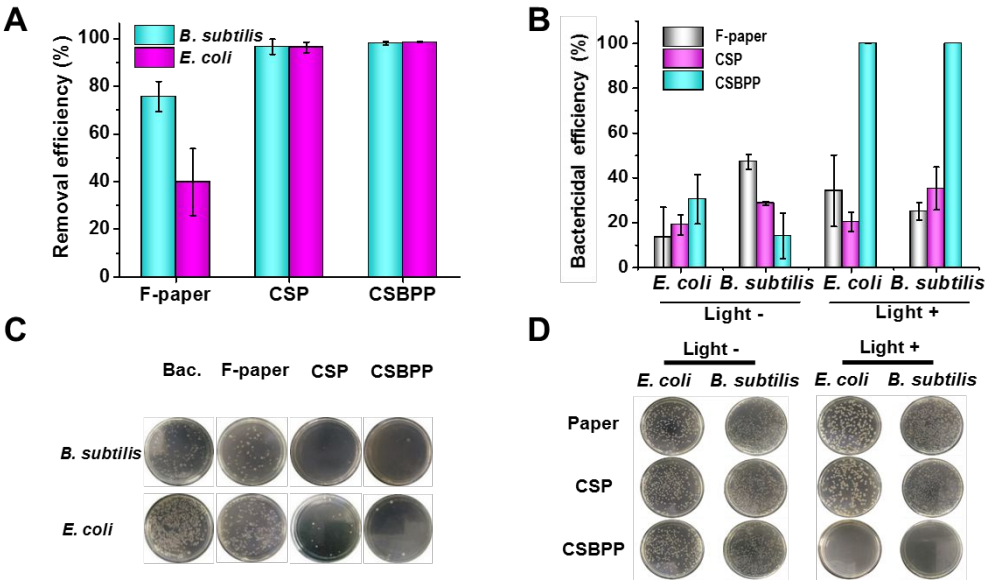

Figure 3. Removal efficiencies (A) and the corresponding CFUs (C) of *B. subtilis* and *E. coli* treated by the F-paper, CSP, and CSBPP. Bactericidal efficiencies (B) and the corresponding CFUs (D) of *B. subtilis* and *E. coli* after different treatments with 10 min of NIR illumination.

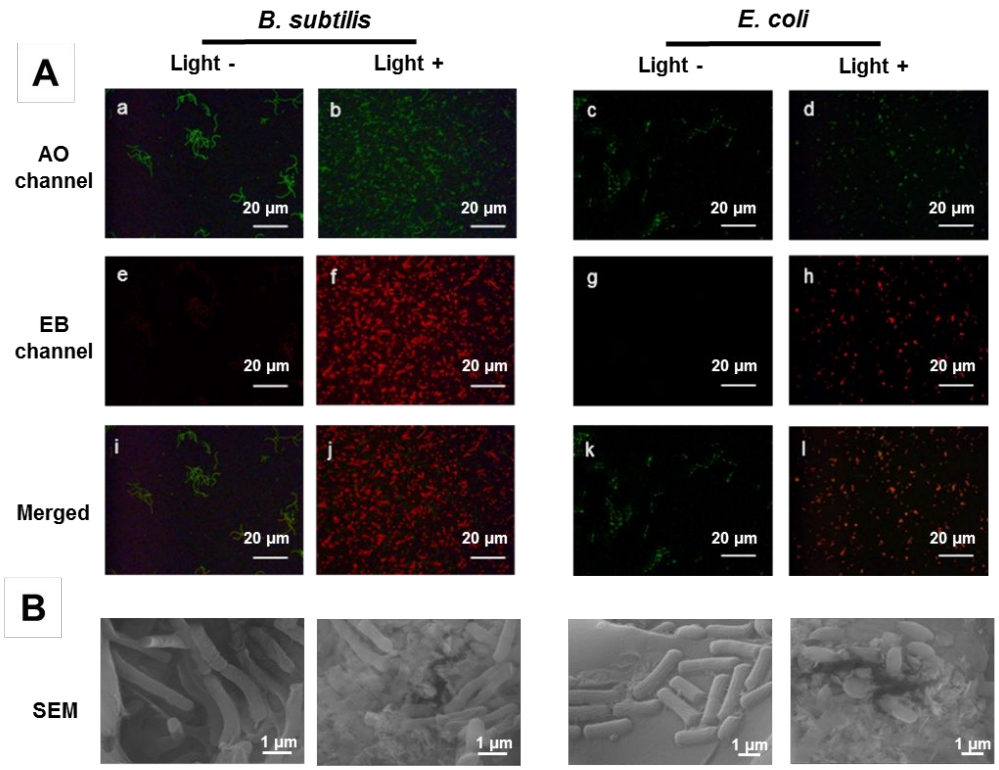

Figure 4. (A) Fluorescence images of AO/EB-stained *B. subtilis* and *E. coli* after treatment with CSBPP in the presence or absence of NIR light. (B) Morphologies of bacterial cells on CSBPP before and after NIR illumination. In (A): green (AO) represents both live and dead bacteria, and red (EB) represents dead bacteria.

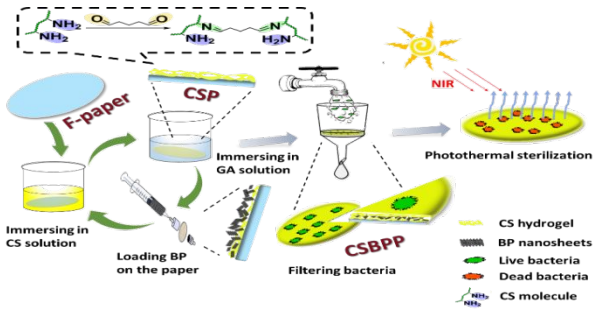

A sandwich-structured filter system embedded with black phosphorus was efficient for NIR-triggered water disinfection.